Journal of
Bioengineering & Biomedical Science

Zhai et al., J Bioengineer & Biomedical Sci 2016, S3
DOI: 10.4172/2155-9538.S3-004

Research Article Open Access

A Neural Control Model for Horizontal Visual, Auditory and Auditory-Visual Bisensory Stimuli Elicited Saccades

Xiu Zhai, Chengqian Che, Benjamin D Mazzarese, Allison V Colberg and John D Enderle*

Department of Biomedical Engineering, University of Connecticut, Storrs, Connecticut 06269-3247, USA

Abstract

To provide a comprehensive investigation of goal-oriented saccades, experiments are designed to trigger fast eye movements by different types of targets, including visual, auditory, and auditory-visual bisensory stimuli. Human saccades are recorded using a high speed eye tracking system. Data is analyzed to produce parameter estimates using system identification technique for a 3rd-order linear horizontal saccadic eye movement model. Saccade characteristics are explored and compared. The auditory-visual stimuli provide the greatest saccade accuracy. Auditory saccades show lower peak velocity and longer duration. Saccade latent period is relatively independent of saccade amplitude, but there is a significant reduction in the bisensory saccades. Neural inputs of saccades are estimated and analyzed as well. Auditory saccades exhibit lower agonist pulse magnitude and longer agonist pulse duration. Antagonist onset delay is longer in auditory saccades. Post saccade phenomena are caused by the post-inhibitory rebound burst of the antagonist motoneurons. There is a higher incidence of dynamic overshoot in auditory saccades than visual saccades, with more in the abducting direction than the adducting direction.

Keywords: Saccades; Extraocular muscles; Oculomotor plant; Visual auditory and auditory-visual bisensory stimuli

Introduction

Saccades are fast eye movements that allow the eyes to quickly move from one target or image to another. The eye muscles are among the fastest in the human body, with a 10° saccade taking only 50 ms. The saccadic system can be thought of as a targeting system that is concerned only with accurate and swift eye movements from one target to another. In this paper, we focus on saccades elicited by visual, auditory and auditory-visual bisensory stimuli and ignore how the neural signal is created by the sensors in the system. Our interest is centered on the neural input to the oculomotor plant. Regardless of the sensory input, the neural input to the oculomotor plant is responsible for movement of the eyes so that images are focused on the central one-half degree region of the retina, known as the fovea. Typically, a saccade operates in an open-loop mode, where once started, it moves to its destination ballistically. After the saccade is complete, the system operates in a closed-loop mode to ensure that the eyes reaches the correct destination. This system does not rely on muscle proprioceptors or real time visual feedback to ensure accuracy of movement because the saccades occur too fast. Instead, a complex neural network involving the mesencephalon, cerebellum, brainstem and the cerebrum keeps track of the eye movement.

A typical saccade is shown in Figure 1, with a latent period of approximately 100 ms, amplitude of 10°, and a duration of approximately 60 ms. Saccadic eye movements are conjugate and ballistic, with a typical duration of 30-100 ms and a latency of 100 - 300 ms. The latent period is thought to be the time interval during which the CNS determines whether to make a saccade, and, if so, calculates the distance the eyeball is to be moved, transforming retinal or auditory errors into transient muscle activity. Also shown in this figure is the velocity of the saccade with a peak velocity of approximately 400°s^{-1} (Figure 1).

Generally, saccades are extremely variable, with wide variations in the latent period, time to peak velocity, peak velocity, and saccade duration. Furthermore, variability is well coordinated for saccades of the same size; saccades with lower peak velocity are matched with longer saccade durations, and saccades with higher peak velocity are matched with shorter saccade durations. Thus, saccades driven to the same destination usually have different trajectories.

To appreciate differences in saccade dynamics, it is often helpful to describe them with saccade main sequence diagrams [1-5]. The main sequence diagrams plot saccade peak velocity–saccade amplitude, saccade duration–saccade amplitude, and saccade latent period–saccade amplitude. Examples of these diagrams are illustrated later in the paper for each stimulus. The saccade size or amplitude is the angular

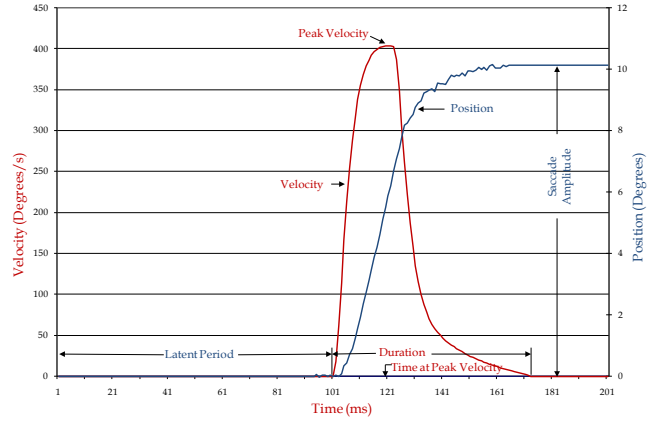

Figure 1: A 10° saccade with various indices labeled.

***Corresponding author:** John D Enderle, Department of Biomedical Engineering, University of Connecticut, 260 Glenbrook Road, Storrs, Connecticut 06269-3247, USA, Tel: +1 860-486-5521; E-mail: jenderle@bme.uconn.edu

Received January 17, 2015; **Accepted** December 22, 2015; **Published** January 28, 2016

Citation: Zhai X, Che C, Mazzarese BD, Colberg AV, Enderle JD (2016) A Neural Control Model for Horizontal Visual, Auditory and Auditory-Visual Bisensory Stimuli Elicited Saccades. J Bioengineer & Biomedical Sci S3:004. doi:10.4172/2155-9538.S3-004

displacement from the initial position to its destination. The size of a saccade ranges from less than a degree (microsaccades) to 45° in both the nasal (toward the nose) and temporal (toward the temple) directions. Peak or maximum velocity occurs at approximately half the duration of the saccade for small saccades less than 15° [1]. The duration of a saccadic eye movement is the time from the start to the end of a saccade. Duration is usually difficult to determine from the saccade amplitude vs. time graph, but it is more easily seen in the velocity vs. time graph as shown in Figure 1. Saccade durations are approximately 30-40 ms for saccades less than 7, and up to 100 ms for large saccades. For saccades greater than 7°, there is a linear relationship between saccade amplitude and duration [4,5]. For saccades less than 7°, the duration is approximately constant vs. saccades amplitude [4,5]. The latent period is the time interval from when a target appears until the eyes begin to move and is relatively independent vs. saccade amplitude [4,5].

Voluntary saccades are often made in response to sensory inputs. Visually elicited saccades (V-saccades) have been investigated extensively, including the oculomotor plant and the neural signals that drive the eye movements [4-13]. Saccade responses to auditory (A-saccades) and auditory-visual combined (AV-saccades) stimuli have been presented in the literature that primarily focused on auditory saccade accuracy and latency [14-23]. Some have reported that the latent period of auditory saccades decreases with increasing target eccentricity [14-18] or at least is greater in small saccade degrees than in larger saccades [19]. By comparing saccades that are triggered by different types of stimuli, a significant reduction of latent period is found in auditory-visual bisensory saccades [20,22,23]. It has also been shown that auditory saccades have lower peak velocity, longer latency, longer duration and are less accurate than visual saccades [19,21]. The mechanism that explains the differences in saccade characteristics to visual, auditory, and auditory-visual bisensory stimuli is still unknown, and is the subject of this paper. In addition to the investigation of saccade characteristics, many studies focus on modeling eye plant dynamics in response to saccade controllers. The work provided in this paper is based on a linear 3rd-order model of the oculomotor plant for horizontal saccades by Enderle et al. [5-13].

The oculomotor plant shown in Figure 2 consists of the eyeball, a passive Voigt element (a viscosity and elasticity element in parallel), and two extraocular muscles, where the rectus muscle is modeled by a Voigt element in series with another Voigt element in parallel with an active state tension generator [4,5,12]. The muscle model in Figure 2 has accurate nonlinear force-velocity and length-tension relationships that agree with the data [4,5,6,12]. We refer to the rectus muscle model in Figure 2 as a whole muscle model.

The inputs to the muscle are the agonist and antagonist active-state tensions, which are derived from a low-pass filtering of the saccadic neural innervation signals. The neural inputs are described by pulse-slide-step waveforms with a post inhibitory rebound burst (PIRB) as shown in Figure 3. The neural controller is based on a time-optimal controller [4,5,7,9,24]. The PIRB in the antagonist motoneurons causes the post-saccade phenomena, called a dynamic overshoot or a glissade. The oculomotor plant and neural controller involve a total of 25 parameters that are estimated by the system identification technique [4,5]. The system identification program is written in FORTRAN, with initial parameter estimates and data as input to a conjugate gradient iteration process, to determine the final parameter values [4-6]. Details about the FORTRAN program and the system identification technique are provided in Enderle and Zhou [4,5].

In agreement with the time-optimal saccade controller, Enderle et al. presented the neural input properties for visual goal-directed saccades [4-6,9,12,13,24]. Agonist pulse magnitude remains approximately constant for saccades over 7°, while a linear increase is observed for saccades less than 7°. While saccades less than 7° appear not to be time-optimal, in fact they are since the neurons fire maximally and the number of neurons firing increases as saccade amplitude increases. For saccades of the same amplitude, a great variability is observed in the pulse magnitude estimates. At the same time, the agonist pulse duration increases as a function of saccade amplitude for large saccades, and it is relatively constant in small saccades. Saccades with a dynamic overshoot or glissade have a more notable rebound burst and PIRB occurs with great randomness [4,5]. There are more saccades with dynamic overshoot in the abducting than adducting direction, and the PIRB magnitude for dynamic overshoots are usually larger than that for glissades, while the duration of PIRB is approximately 12 ms.

The whole muscle model shown in Figure 2 was recently updated with a muscle fiber muscle model shown in Figure 4 that has the same characteristics of the whole muscle model, with accurate nonlinear force-velocity and length-tension relationships that agree with the data [8,13]. The importance of this new muscle fiber muscle model is that each muscle fiber has its own neural input. Operating within the oculomotor plant in Figure 4, the time-optimal controller described previously by Enderle et al. [4,5,12] now accurately depicts the true state of the controller where individual agonist neurons fire maximally during the agonist pulse independent of eye position, while the antagonist muscle is inhibited [8,13]. Only the number of agonist neurons firing maximally and the agonist pulse duration determine the saccade amplitude. This theory has been fully examined with the static and dynamic behaviors in excellent agreement with experimental data. The estimates of the neural controller also provide an excellent match with the burst-tonic neuron data in the monkey [10,13]. The study described in this paper provides a more comprehensive investigation of saccades induced by visual, auditory and auditory-visual bisensory stimuli by describing a comprehensive neural controller, and expands on our previous work [25,26].

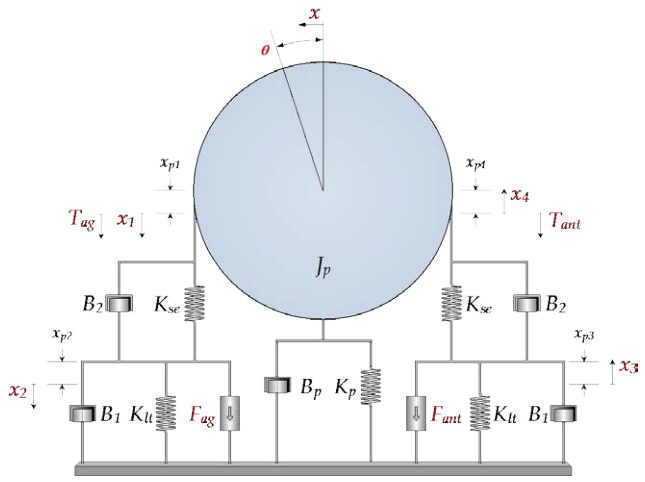

Figure 2: Oculomotor plant with a whole muscle model.Model parameters *B* are viscous elements, *K* are elastic elements, *J* is a moment of inertia, and *F* are active-state tension elements. θ represents the angle that the eyeball is rotated,*x* represents the length of arc rotated, and *x*,are changes from equilibrium from the nodes.Refer to [4]for further description of the model elements.

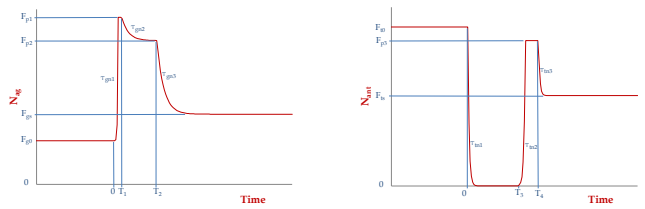

Figure 3: Neural input to the horizontal saccade system. (Left) Agonist input. (Right) Antagonist input. Refer to [4] for further description of the inputs.

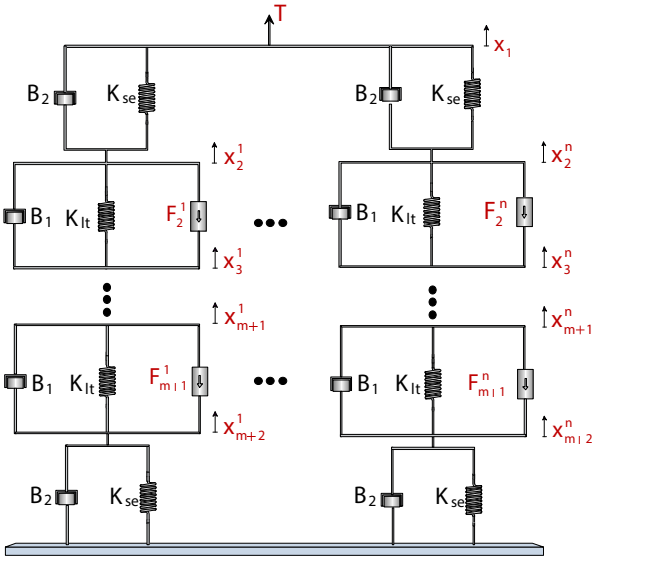

Figure 4: Muscle fiber model of muscle. Model parameters *B* are viscous elements, *K* are elastic elements, and *F* are active-state tension elements. Variables *x* are changes from equilibrium from the nodes and *T* is the tension created by the muscle. Refer to [8,13] for further description of the model elements.

Materials and Methods

Subjects

Four subjects, two males and two females, aged 20-26, participate in this study. None of the subjects disclose any history of visual, auditory or vestibular disorders, and none are taking any medications known for CNS illness. One male and one female have dark colored eyes while the other two have light colored eyes. All subjects demonstrate normal visual and auditory functions.

Apparatus

All the tests are performed in an independent, quiet room with normal illumination. The experiments are conducted using custom written software and data is collected using an iView X™ system, a high speed eye tracking device by Senso Motoric Instruments (SMI).

The visual targets consist of white solid dots (4 mm diameter) on a gray background displayed on a 30" computer monitor in front of the subject. Nine target positions are presented to the subject at angles of 0º, 5º, 10º, 15º and 20º from the center to left or right in the horizontal plane. The distance between the screen and the subject is 830 mm.

The auditory targets are tone signals. The frequency of the sound is 1kHz. With an average intensity around 60dB SPL. To coordinate the sound sources with visual stimuli, 3D positional audio is used for the tests, and implemented using H3D Binaural Spatializer plug-in (by Longcat Audio Technologies) inserted in audio editing software (Adobe Audition CS5.5). The sound source locations are exactly the same as the visual stimuli locations. All the auditory stimuli are heard by a Bose stereo headphone, which electronically identifies and reduces the unwanted noise around the subjects, as well as implement the acquisition of the 3D sound sources.

The timing of the stimulus events is controlled by the Experiment Center™ from SMI. Visual and auditory stimuli are presented either alone or synchronously, depending on the experiment. Eye movements are recorded using the iView X™ system, which consists of an eye tracker (1250 Hz sample rate) and a computer workstation. The workstation controls the camera equipment, and at the same time, processes all eye video signals from the experiment. Moreover, stimulus events presented with the Experiment Center™ are synchronized with data collected by the iView X™ workstation. The data is recorded and stored automatically by the system, then converted and exported to a text file, which contains pupil size and position, gaze position, detected saccades and fixations.

Experiment design

A typical experiment for recording saccades has the subject sitting before a horizontal target display [7]. A saccade is made by the subject when the active target is switched off and another target is switched on. The subject is instructed to maintain their eyes on the target by moving their eyes as fast as possible. Subjects are tested under three tracking conditions. In V-saccade, only a visual stimulus is presented. Subjects respond to each target movement, and a saccade is made when the dot disappears at one position and appears at another position. In AV-saccade, visual and auditory stimuli are provided together and move synchronously; the subjects respond to both stimuli. In an A-saccade, the target starts at the center with both the visual and auditory stimuli presented. Then the auditory stimulus is displayed alone at a peripheral position without any visual cue, and the stimulus screen is blank at this time. Subjects respond after they hear the sound onset to locate the position of the source as soon as possible.

The targets are presented in a same sequence in the three experiments (V-saccade, AV-saccade and A-saccade), with parts of each experiment, which triggered 5º, 10º, 15º and 20º saccades, respectively. The target presentation starts at the center position, and then moves to a peripheral position. Next, the fixation point appears at the center again, followed by another movement to the right or left, etc. Only the saccades that move from center to a peripheral position are analyzed. The duration of any single stimulus presentation is random from 3000 ms to 5000 ms.

Data processing and analysis

Raw data contains pupil and gaze information is generated automatically by the iView X™ system. Gaze data from the left eye is recorded in pixels, and then converted to degrees. The converted eye position data is plotted in Microsoft® Excel for a quality examination, and then parameter estimation takes place as described by Enderle et al. on acceptable saccades [4-6].

A FORTRAN program is used to compute parameter estimates for the models of horizontal saccades as illustrated in Figure 2 and 5. The data set of 1,511 saccades is the largest study of saccades that includes estimation of the neural input for the three different stimuli. Final estimates of model parameters are found using a system identification

technique. Saccade characteristics and neural inputs are also estimated, and post-saccade phenomena are analyzed.

Results

Based on the data quality and initial condition requirements, approximately 35% of the collected data is discarded [4-6]. The analyzed data consists of 486 V-saccade, 457 AV-saccade and 568 A-saccade that are successfully analyzed by the FORTRAN program. Despite the variation between subjects, the result obtained are highly consistent with each other. One subject's data is presented in this paper for analysis and discussion. The other subject's results are similar in nature.

Saccade main sequence characteristics

The main sequence diagrams of V-saccades, AV-saccades and A-saccades are shown in Figure 6. Shown in Figure 7 are regression curves for the three inputs plotted together for comparison. The data is for adduction saccades, while abduction saccades are similar.

Peak velocity increases exponentially with increasing saccade amplitude. Data is fitted to the equation

$$v = \alpha\left(1 - e^{-\frac{x}{\beta}}\right) \quad (1)$$

Where v is the peak saccade velocity, x is the saccade amplitude, and the constants α and β are evaluated to minimize the summed error squared between the curve and the data [2]. The parameter values for α and β are listed in Table 1. As shown in Figure 6 (Top), the V-saccade peak velocity is slightly larger than the AV-saccade, which typically has peak velocity from 100 degrees per second up to 500 degrees per second. Comparatively, the A-saccades have a lower peak velocity. The exponential shape of the peak velocity vs. saccade amplitude is consistent with others reported in the literature [1-3].

Enderle et al. recognized that the duration of a saccade is more complex than originally envisioned [4,5,9]. For saccades greater than 7°, there is a linear relationship between saccade amplitude and duration [4,5]. For saccades less than 7°, the duration is approximately constant vs. saccades amplitude [4,5]. Thus, the analysis and regression analysis for the duration data are carried out in two intervals, one under 7°, and one for those greater than 7°. As shown in Figure 6 (Middle), V-saccade and AV-saccade duration is approximately constant for saccades under

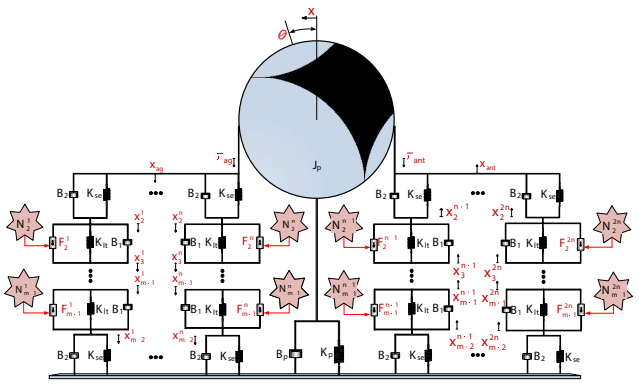

Figure 5: Oculomotor plant for horizontal saccades with a muscle fiber muscle model for the agonist and antagonist rectus eye muscles. Model parameters are described in Figure 4, and J is a moment of inertia. θ represents the angle that the eyeball is rotated,x represents the length of arc rotated, and τ is the torque.

	V-saccade		AV-saccade		A-saccade	
Direction	-	+	-	+	-	+
α	538	457	497	431	416	365
β	9.7	6.2	5.8	6.1	4.1	4.4

Table 1: Parameter estimates for peak velocity vs. saccade amplitude. (* '-' is to left (abduction) and '+' is to right (adduction).

7°, which is around 30-40 ms, while it is linearly proportional to saccade amplitudes up to 80 ms for saccades above 7°. For small A-saccades, the slope of the regression line is larger than that in V-saccades and AV-saccades. For larger A-saccades, the slope of the regression line is larger than V-saccades and AV-saccades as well. The A-saccade duration ranges from 30 ms to 100 ms, and is longer for especially large saccades as compared to the other two stimuli.

The latent period verses saccade amplitude is shown in Figure 7 (Bottom). The overall results indicate that the latent period is relatively independent of saccade amplitude. In each stimulus condition, there is a slight increase in mean latent period with saccade amplitude, but A-saccade shows a great variability between 100 and 300 ms. In general, there is a significant reduction of latent period in AV-saccade, which is from 100 ms to 200 ms. Figure 7 shows a summary of the saccade main sequence characteristics of those illustrated in Figure 6.

Neural input estimation and saccade simulations

Graphs in Figure 8 are based on parameter estimates calculated by the system identification technique for anV-saccade, AV-saccade and A-saccade of different sizes for a normal saccade (a), glissadic saccade (b), and a saccade with dynamic overshoot (c). The accuracy demonstrated in this graph is consistent with the other 1,508 saccades analyzed.

The estimated agonist and antagonist neural inputs, N_{ag} and N_{ant}, and active-state tensions, F_{ag} and F_{ant}, are presented in the first two rows for the three saccades. Notice that the small saccade has a lower agonist pulse magnitude than the other two larger saccades in the first row. The post inhibitory rebound burst (PIRB) is also evident in the second row for (b) and (c). The 10° AV-saccade shown in Figure 8(b) illustrates a glissade that is caused by a PIRB in the antagonist neural input. Figure 8(c) shows a 15° A-saccade with a dynamic overshoot that is caused by a larger PIRB in the antagonist neural input.

For all 1, 511 saccades, the model predictions match amplitude data and data-calculated velocity (derivative of the amplitude) and data-calculated acceleration (second derivative of the amplitude) very well. The three saccades presented in rows three to five are illustrative of the results for all saccades. The acceleration estimated from the model is least accurate when compared to the second derivative of the amplitude data, but it should be noted that the estimate of the second derivative considerably amplifies the noise in the data [7].

Agonist pulse magnitude and duration

As illustrated in Figure 3, the overall agonist pulse occurs in the interval 0-T_2, with a peak magnitude F_{p1}. The results of the system identification parameter estimation are shown in Figures 9 and 10. In each type of saccade, agonist pulse magnitude shows a linear increase from 0.5N to 1.5 N for small saccades less than 7°. For saccade amplitudes greater than this, the pulse magnitude is relatively constant. Agonist pulse duration remains constant at around 10 ms for small saccades less than 7°. There is a linear increase for larger saccades. These results are true for all three inputs. Figure 10 shows a summary regression graphs for the results illustrated in Figure 9.

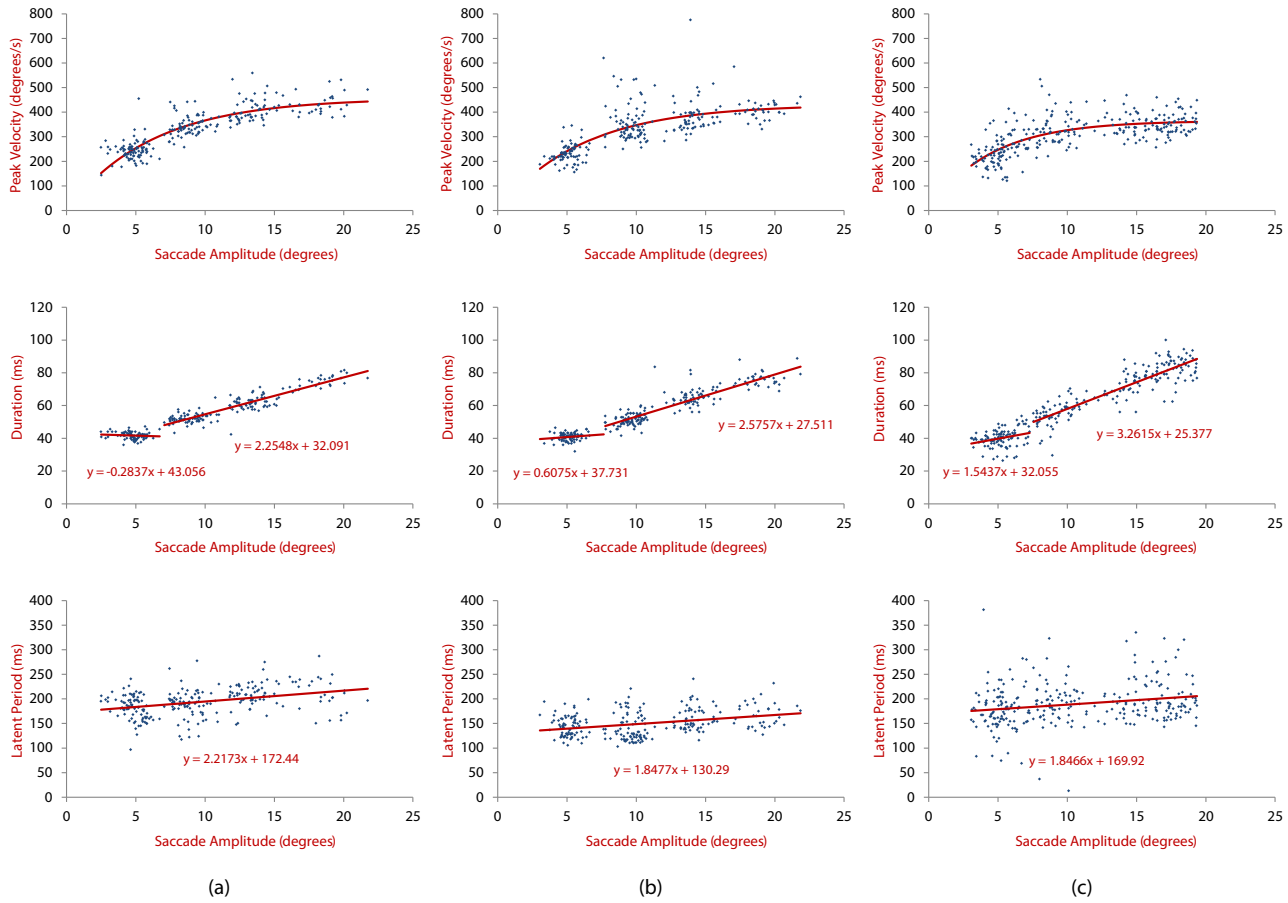

Figure 6: Main sequence diagrams for human saccades. (Top) Saccade peak velocity vs. amplitude. (Middle) Saccade duration vs. amplitude. (Bottom) Saccade latent period vs. amplitude. (a) V-saccade. (b) AV-saccade. (c) A-saccade.

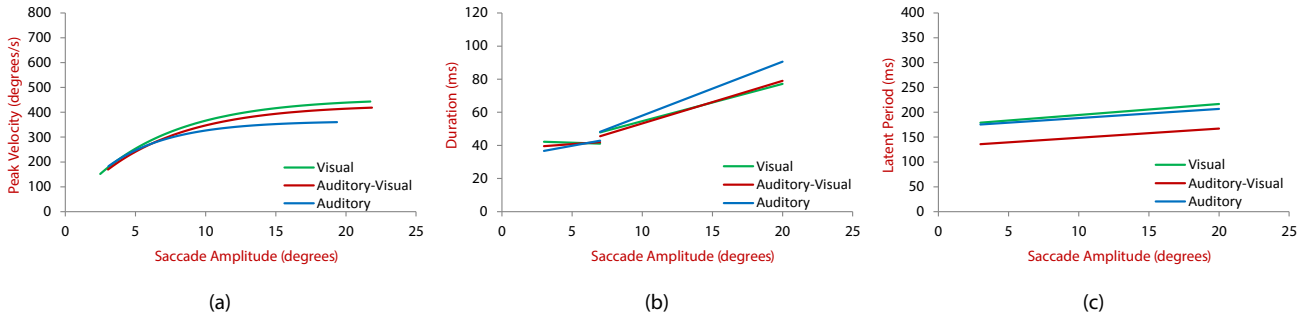

Figure 7: Regression fits for main sequence diagrams. (a) Saccade peak velocity vs. amplitude. (b) Saccade duration vs. amplitude. (c) Saccade latent period vs. amplitude.

When compared, the regression fits in both abduction and adduction saccades has the following characterizations:

- A-saccades exhibit lower agonist pulse magnitude and longer agonist pulse duration in saccades between 12° and 20°.
- V-saccades have a slight lower pulse magnitude in small saccades less than 7° according to the regression fit. Visual inspection indicates that this result is skewed by a few data points.
- For saccades approximately 10°, AV-saccades show slight higher pulse magnitude than the other two types.

Post-inhibitory rebound burst in antagonist motoneurons from auditory stimuli

Figure 11 shows the estimates for the PIRB in the antagonist motoneurons of an A-saccade, where the PIRB induces a reverse peak velocity, with features similar to the V-saccade and AV-saccade. This is the first time PIRB auditory induced saccades have been presented in the literature, with a complete description of the neural input.

Figure 11(a) shows the relationship between PIRB magnitude (F_{p3} in Figure 3) and saccade amplitude. Saccades with dynamic overshoots have a larger PIRB magnitude that is between 0.3-0.6N, while saccades with glissades have PIRB magnitude between 0.3-0.45N. As shown in Figure11(b), PIRB duration (T_4-T_3 Figure 3) for dynamic and glissadic overshoots falls within 8-14 ms, with considerable variation for the same saccade amplitude.

In Figure11(c) and 11(d), antagonist onset delay (T_3-T_2 in Figure 3) is plotted against saccade amplitude, as well as PIRB magnitude. Antagonist onset delay is typically 2-35 ms, and small saccades have shorter onset delay, while large saccades have a longer onset delay. Antagonist onset delay is longer in A-saccades compared with the V-saccades and AV-saccades of the same size. At the same time, the antagonist onset delay vs. PIRB magnitude are clustered closer to the origin for normal saccades, while glissades cluster in a band followed by saccades with a dynamic over shoot while moving further from the origin.

Post-saccade behavior

Table 2 shows statistics for post-saccade phenomena. Either a dynamic overshoot or a glissadic overshoot occurs in 50.4% of the V-saccades, 65.65% of the AV-saccades, and 76.76% of the A-saccades. Approximately 65% of all the saccades recorded contain a post-saccade phenomenon that occurs quite randomly.

There is a higher incidence of overshoot, especially dynamic overshoot, in A-saccades. Moreover, dynamic overshoot occurs more often in the abducting direction than the adducting direction saccades. Left eye A-saccades with dynamic overshoot occurred in 72.64% in the left direction saccades, while only 29.29% occurred in the right direction. In V-saccades and AV-saccades, overshoot incidence is also observed in the data.

Discussion

Saccade characteristics

The results of this study continue to support most of the main sequence diagrams in agreement with other studies, except for a new interpretation on saccade duration for small saccades less than 7°, which is a constant. The characteristics of V-saccade and AV-saccade are quite similar. This is because visual targets are much easier to follow than auditory targets. Subjects seem to react to and locate the stimuli's positions more easily with visual targets, which are the dominant stimuli. The addition of an auditory stimulus to a visual stimulus did not significantly improve performance.

	V-saccade	AV-saccade	A-saccade
Total Number	486	457	568
Normal Saccade	241 (49.59%)	157 (34.35%)	132 (23.24%)
Dynamic Overshoot	157 (32.30%)	195 (42.67%)	309 (54.4%)
Glissadic Overshoot	88 (18.11%)	105 (22.98%)	127 (22.36%)

Table 2: Statistics of post-saccade phenomena.

The studies of Zahn et al., Engelken et al. and LaCroix et al. demonstrates that auditory saccades are slower with a lower peak velocity and longer in duration, as well as being less accurate than visual saccades [18-20]. Our results are in agreement with these conclusions. We find that the auditory stimuli produce saccades with 10% - 20% lower peak velocity and approximately 15% longer duration than visual and auditory-visual bisensory stimuli triggered saccades, especially for larger saccades.

Saccade velocity is related to the size of the population of the active superior colliculus neurons that execute a saccade [4,12,13,27,28]. Fewer cells in the superior colliculus respond to sound stimuli, thus the saccades have a lower peak velocity and longer duration [29-33].

Interpretations of the saccade latent period are complicated. The slight increase of latent period with saccade amplitude in V-saccades is consistent with the previous studies by Zahn et al., and Engelken et al. [18-20]. However, in our A-saccade results, there is no obvious decrease of latency with increasing target eccentricity as presented by others [14-18]. In previous studies by Frens et al. and Gabriel et al. a significant long latency is found only in small saccades under 10 degrees, while the average latency was relatively constant in larger saccades [14,15]. We find a great variability in the A-saccade latent period, and that it is independent of saccade amplitude. This may be because the detection of sound onset is faster than visual stimuli for humans, but it may require more processing time to accurately locate the sound source. Possibly, the presentation and properties (intensity and frequency) of the auditory signals influence the performance of the subjects [14]. In general, AV-saccades show a significant reduction in latent period, perhaps because the sound acts as a cue to improve the response time. Similar results are present in the results by Bell et al., and Corneil et al., in both high- and low-intensity stimuli conditions [22,23].

As shown in Figure 6, saccades are clustered at desired degree positions, which is more obvious in V-saccades and AV-saccades, than the A-saccades. In general, the AV-saccade exhibited the smallest error in saccade accuracy. This was followed by the V-saccade, and the least accurate was the A-saccade.

Agonist neural input

To provide more accurate analysis, we divide the saccades into three groups: saccades under 7°, saccades approximately10°, and saccades larger than 12°. Enderle and Zhou show that in the V-saccade, the estimated agonist pulse magnitude don't significantly increase with increasing saccade amplitude for saccades larger than 12°, but there is a more obvious linear increase for small saccades under 7° [4,5]. Our result is in agreement with these studies for small and large saccade amplitude, consistent with the theory of the time-optimal controller under physiological constraints.

Whole muscle based oculomotor plant

In the model used here, the overall neural input increases as the amplitude of saccades increases up to 7° due to the increasing number of firing neurons, with all neurons firing maximally. In large saccades, all neurons fire maximally, which results in a relatively constant pulse magnitude. This is given by

$$N_{ag} = \begin{cases} N(\theta_T) N_{ag_i} \theta < 7^\circ \\ N_{ag_{\max}} \theta \geq 7^\circ \end{cases} \quad (2)$$

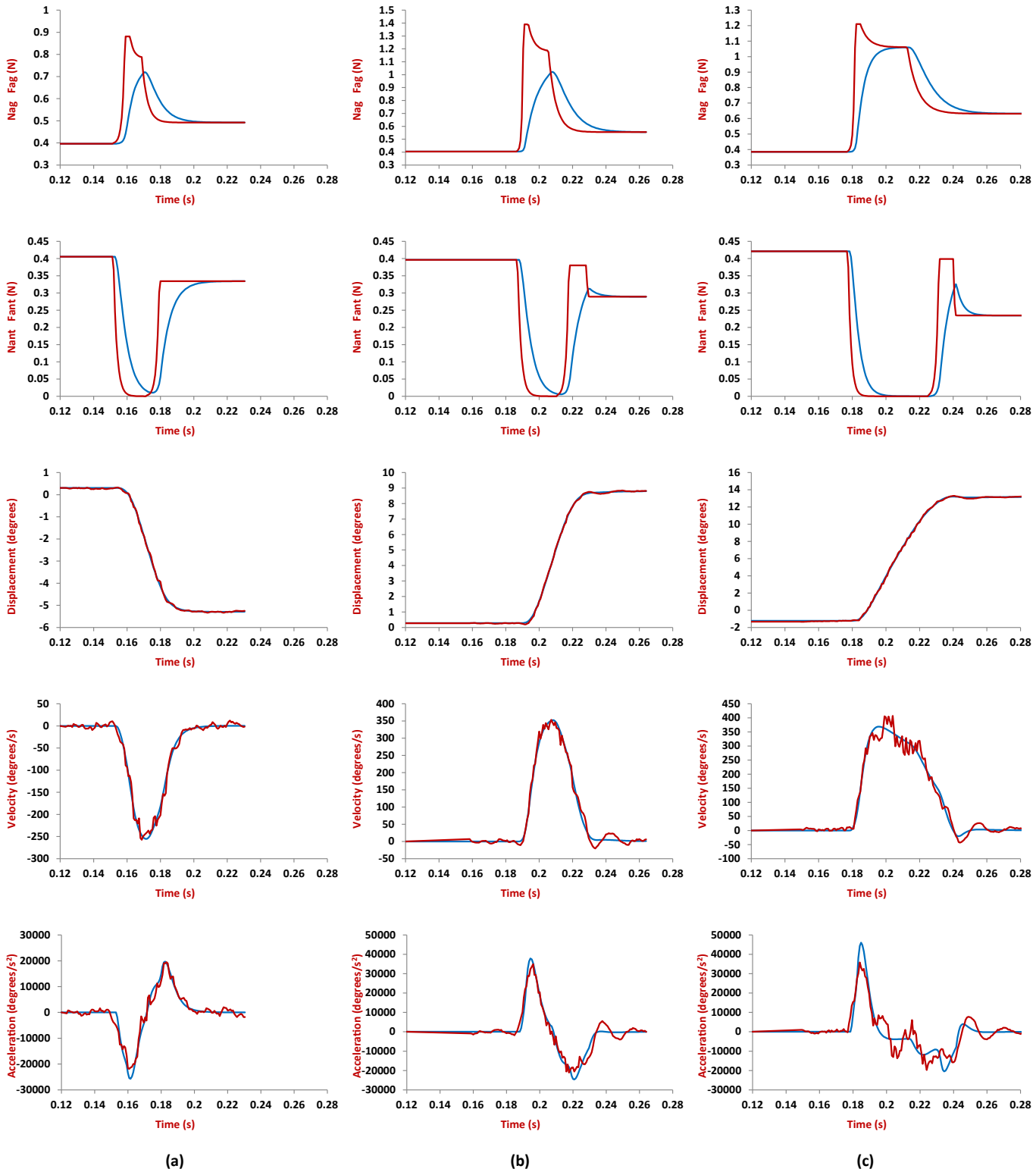

Figure 8: Model estimated neural inputs Nag and Nant (red line), active-state tensions Fag and Fant(blue line) of three saccades. Also shown are the model predictions using the parameter estimates from the system identification technique for amplitude, velocity, acceleration (blue line), and the experimental data (red line). (a) Normal 5° V-saccade. (b) 10° AV-saccade with a glissade. (c) 15° A-saccade with a dynamic overshoot.

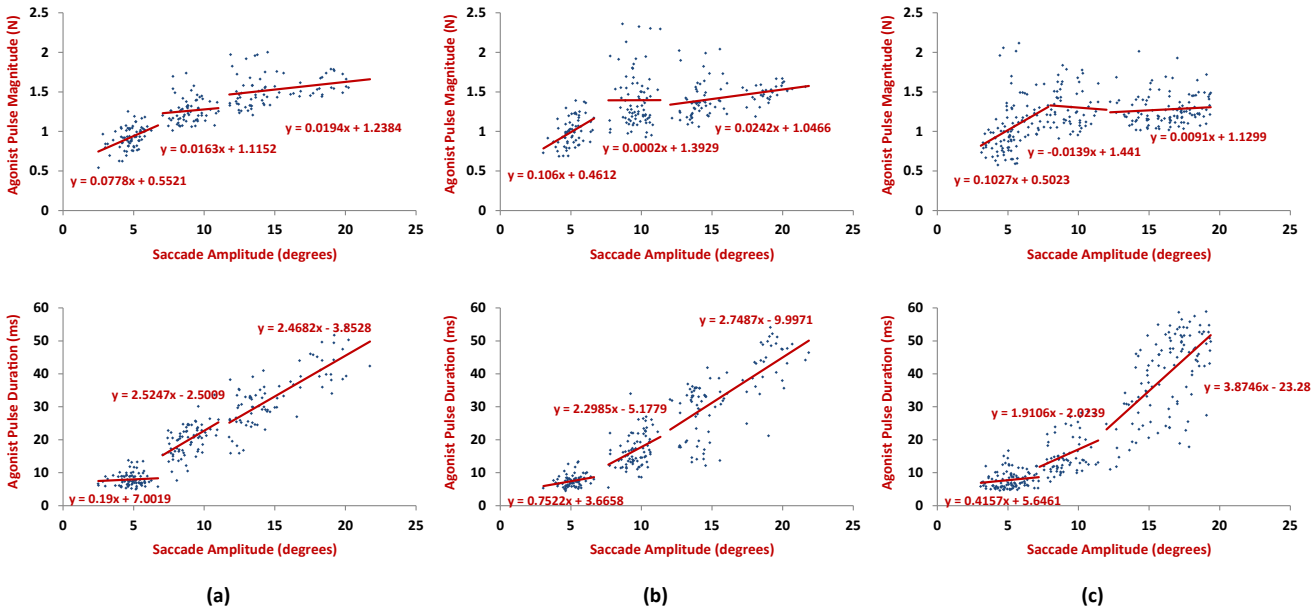

Figure 9: Agonist pulse magnitude (Top) and duration (Bottom) as functions of saccade amplitude. (a) V-saccades. (b) AV-saccades. (c) A-saccades.

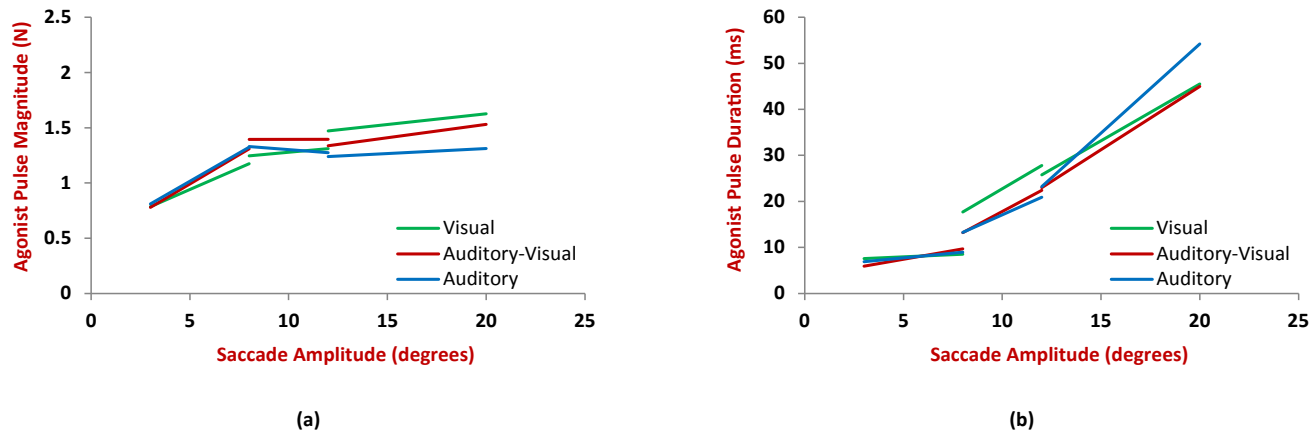

Figure 10: Agonist neural input regression fits for V-saccades, AV-saccades, and A-saccades. (a) Agonist pulse magnitude vs. saccade amplitude. (b) Agonist pulse duration vs. saccade amplitude.

Where $N(\theta_T)$ is the number of neurons firing for a saccade of θ_T degrees, N_{agi} is the contribution from an individual neuron, and $N_{ag\,max}$ is the combined input from all neurons.

Here, we also examine the V-saccades of approximately 10° (Figures 9(a) and 10(a)). The agonist pulse magnitude is also relatively constant, but the average value is slightly lower than larger saccades above 12°. This result is consistent with the recent muscle fiber model, that is, 12° saccades generally have fewer active neurons than the 16° and 20° saccades [8]. The human data presented here supports a movement field of activity in the superior colliculus that continues to increase up to 12° [4,5].

In an A-saccade, not many saccades have an agonist pulse magnitude that is less than 0.5 N, as presented by LaCroix et al. [19]. The results from LaCroix et al. were generated from an earlier version of the FORTRAN program that used a simple pulse-step for the agonist pulse rather than the more accurate neural input shown in Figure 3 used here. We still find that for large saccades, A-saccades have a lower agonist pulse magnitude than visual saccades,

which is less than 1.2 N (Figure 10(a)). This phenomenon exists because a smaller population of neurons firing in the superior colliculus (SC) during an A-saccade than a V-saccade [19,29-33].

For small saccades, agonist input is related to the number of agonist neurons maximally firing for all stimuli. Since smaller saccades have fewer agonist neurons firing than larger saccades, the firing synchrony of individual neurons has a greater impact on the overall neural input for small saccades [13]. Any lack of synchrony causes the overall agonist

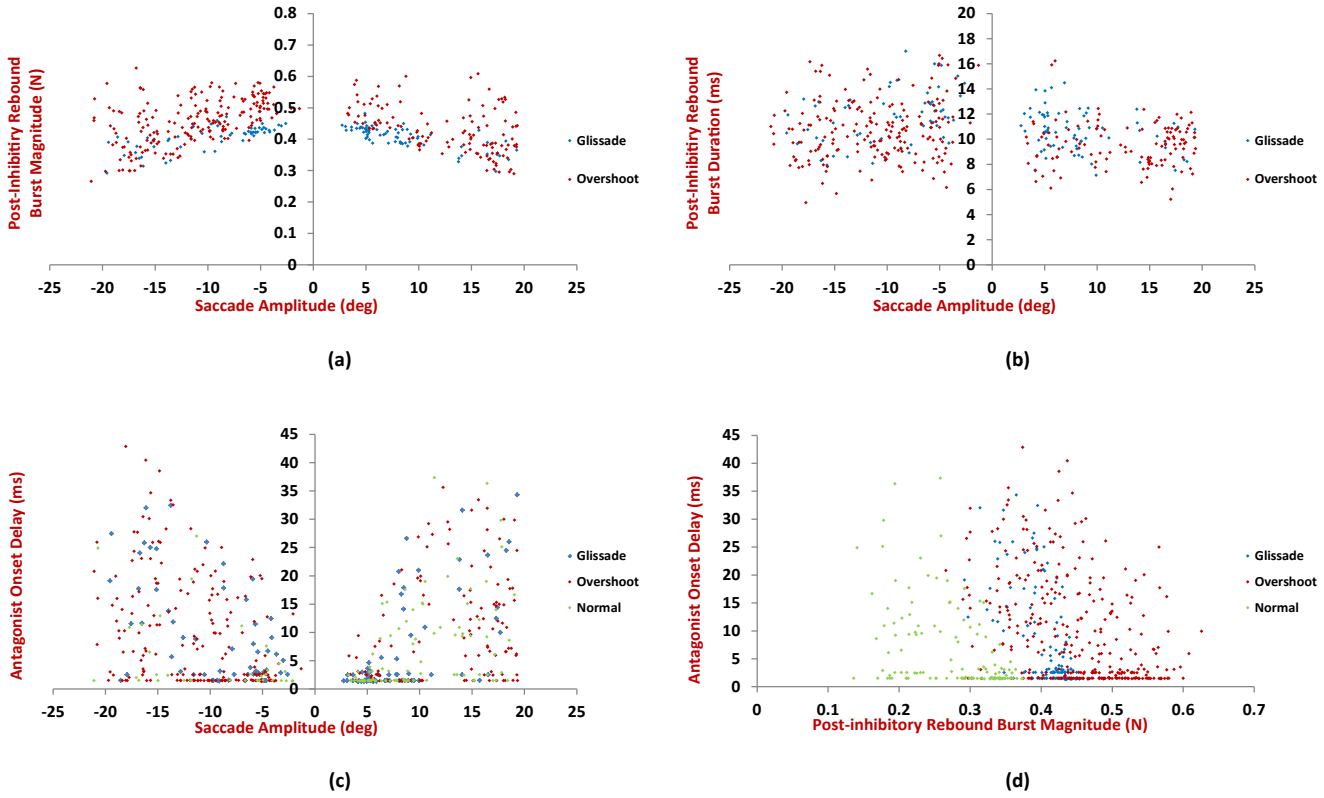

Figure 11: Antagonist neural inputs and post saccade phenomena in A-saccade. (a) PIRB magnitude vs. saccade amplitude. (b) PIRB duration vs. saccade amplitude. (c) Antagonist onset vs. saccade amplitude. (d) Antagonist onset delay vs. PIRB magnitude.

input to be smaller. V-saccades less than 7° show a slight lower pulse magnitude than A-saccades. This indicates that the neurons responding to sound cues are more likely to start firing together at the same instant.

The deep layers of the superior colliculus (dSC) initiate a saccade based on the distance between the current position of the eye and the desired target. The neural activity in the SC is organized into movement fields that are associated with the direction and saccade amplitude. Multisensory neurons are abundant in dSC that handle different simultaneous sensory modalities (e.g., visual, auditory, somatosensory) [15,30,31,34]. By responding to stimuli from more than one modality and projecting to downstream motor centers, the SC coordinates the different sensory modalities. At the SC level, visual and auditory inputs are converted into a single coordinate system which allows a sharing of a common efferent pathway for the generation of saccades [29,30,35]. We propose the SC movement field remains the same for visual and auditory stimuli [30,32-34].

Tightly coordinated with the agonist pulse magnitude, the agonist pulse duration is also consistent with previous studies in which the duration is constant in small saccades while there is a linear increase for large saccades. Our hypothes is that the small saccade pulse duration has a minimum time period that the excitatory burst neurons (EBN) can be switched on and off (a biophysical property of the neuron membrane). Again, it is important to understand that the number of maximally firing agonist neurons and the pulse duration determine the size of the saccade. In terms of control, it is easier to operate the system in this small-large saccade pattern, rather than a changing firing rate for all neurons as a function of saccade amplitude as proposed by others [13]. The system described here is time-optimal based on physiological constraints.

Muscle fiber muscle based oculomotor plant

In Figure 5, the oculomotor plant based on a muscle fiber muscle model is illustrated. The muscle fiber muscle model has been shown to have the static and dynamic characteristics of real muscle, and further has identical performance to that of the whole muscle model [8,10,13]. A complete description of the model, parameter estimation and simulation results have been described by Enderle et al.[8,10,13]. The neural input to the oculomotor plant is a pulse-slide-step that is time optimal, where individual neurons fire maximally during the pulse portion of the saccade, and only the duration of the neuron firing and the number of active neurons determine the size of the saccade. This model is an update of the whole muscle oculomotor plant presented in the previous section.

A unified time-optimal neural controller is proposed for horizontal saccades of all sizes using a muscle fiber model for visual, auditory, and visual and auditory stimuli. Using a value of 1.5 for F_{p1} and a value of 1.3 for F_{p2} based on the results illustrated in Figure 9, the neural input and saccade amplitude are shown in Figure 12. The saccades plotted in Figure 12 are the same saccades illustrated in Figure 8. The blue line for the diagrams on the left in Figure 12 represents the agonist neural input to the muscle fiber muscle, with all active neurons firing maximally. The red line for the diagrams on the left in Figure 12 represents the agonist neural input to the whole muscle, with a neuron firing according to Eq. 2, where small saccades have a lower firing rate than large saccades which fire maximally.

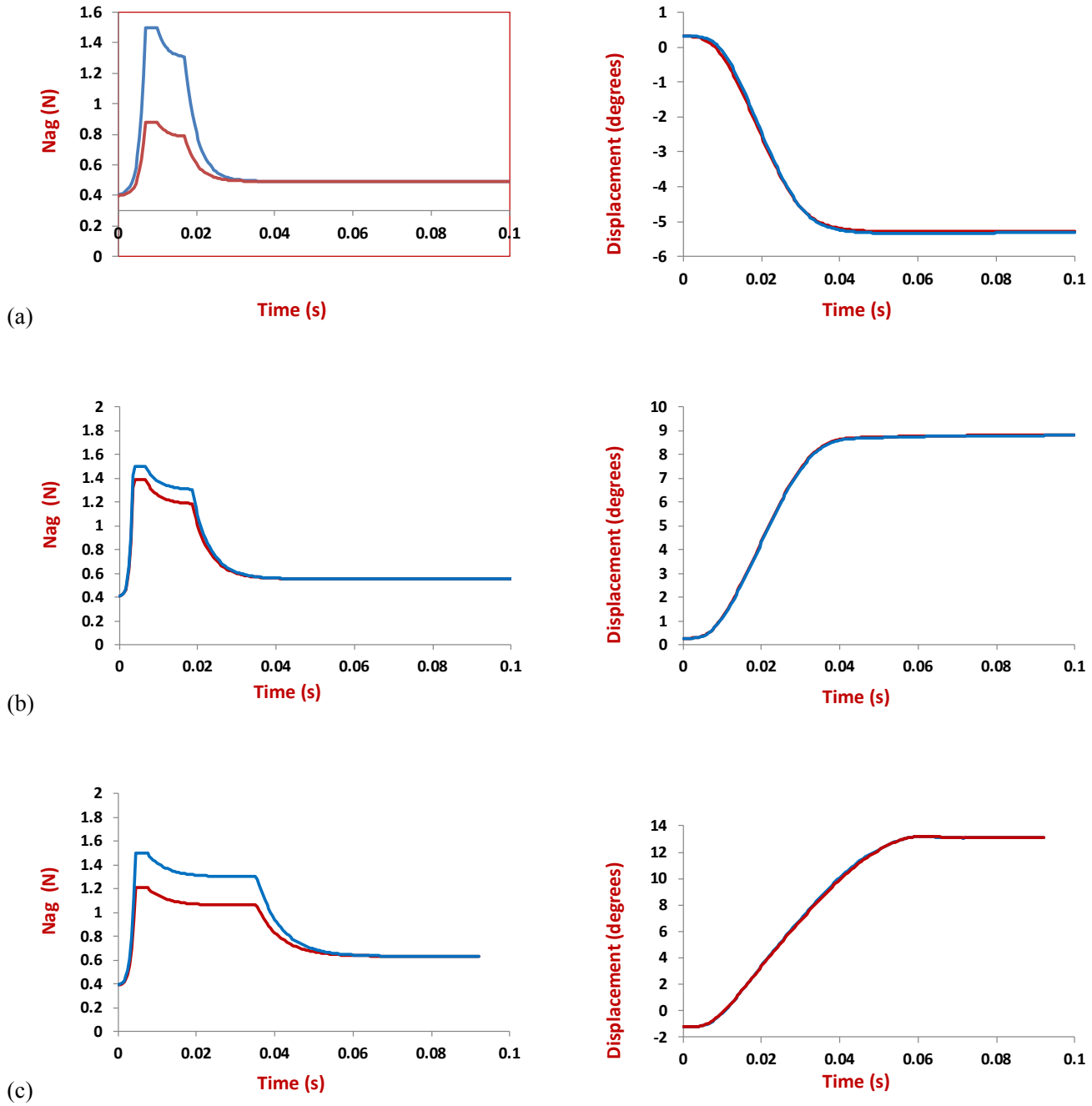

Figure 12: Shown are estimated neural inputs Nagfor the whole muscle model (red line) and the muscle fiber muscle model (blue line) for the three saccades illustrated in Figure 8 on the left. Also shown on the right are the model predictions using the parameter estimates from the system identification technique for amplitude using the neural inputs on the left. (a) Normal 5º V-saccade with 65% of the neurons firing. (b) 10º AV-saccade with a glissade with 92% of the neurons firing. (c) 15º A-saccade with a dynamic overshootwith 83% of the neurons firing. Note the match in (b) and (c) are excellent and it is difficult to discern the two saccades.

The blue line for the diagrams on the right in Figure 12 represents saccade amplitude using the muscle fiber muscle model, where the number of active neurons firing maximally and the duration of the pulse determine the size of the saccade. The red line for the diagrams on the right in Figure 12 represents saccade amplitude using the whole muscle model. Notice that the saccade amplitudes match each other extremely well.

For case (a), a 5º saccade to a visual stimuli in Figure 12, 65% of the neurons are firing maximally with the muscle fiber muscle model, consistent with previous reports [8,10 ,13]. For case (b), a 10º saccade to a combined visual and auditory stimuli in Figure 12, 92% of the neurons are firing maximally with the muscle fiber muscle model. For case (c), a 15º saccade to an auditory stimuli in Figure 12, 83% of the neurons are firing maximally with the muscle fiber muscle model.

As can be seen in Figure10, the pulse magnitude F_{p1} for large (12°-20°) auditory saccades is lower than visual, and auditory and visual saccades, and the number of neurons actively firing during a large saccade is fewest for an auditory saccade, followed by the auditory-visual bisensory saccade, and most for a visual saccade. This means that there are fewer cells in the SC firing in response to an auditory stimulus. Moreover, neurons firing in the SC in response to an auditory stimulus fire much later than the other stimuli with a lower peak velocity and a longer duration as illustrated in Figure 7.

Post saccade phenomena

When a neuron is inhibited and released without stimulus, a high-frequency burst fires and ends after a short period of time [4,5,9,12,13]. Thus, the inhibition of antagonist burst neurons causes a PIRB at the end of a saccade initiating a post saccade phenomenon. Enderle et al. demonstrate that the antagonist PIRB causes a reverse peak velocity during dynamic overshoots or glissades [4,5,12,13]. Our model predictions accurately match the velocity data for the entire saccade as shown in Figure 8, including those with a glissadic or dynamic overshoot.

Similar to the results provided by Enderle et al. more saccades with an overshoot in the abducting direction occur than in the adducting direction [4,19]. Neurons that fire at steady rates during fixation are called tonic neurons (TN). The firing rate of TNs depends on the eye position and is thought to provide the step component to the motoneurons. Excitatory burst neurons (EBN) and inhibitory burst neurons (IBN) are used in the coordination of the eye movement from the left and right side of the brain. The EBNs excite and are responsible for the burst firing while the IBNs inhibit and are responsible for the pause. During an abducting saccade, ipsilateral abducens motoneurons fire without inhibition, while oculomotor motoneurons are inhibited during the pulse phase. Since the IBNs inhibit the antagonist motoneurons, the resumption of TN and PIRB do not begin until after the ipsilateral IBNs stop firing. Moreover, a greater number of inter nuclear neurons exist and operate during an abducting saccade. There is a longer time delay before the resumption of activities in the oculomotor motoneurons after the pulse phase for abducting saccades than adducting saccades, resulting in more overshoots in the abduction direction [4]. This phenomenon occurs more often in auditory saccades.

However, we don't find significant decrease of dynamic overshoot incidence when saccade amplitude increases, but such relationship is shown for glissade. This phenomenon is due to the contralateral TN's firing rate which decreases as ipsilateral saccade amplitude increases. Fewer saccades have sufficiently high PIRB magnitude as saccade amplitude increases to cause PIRB.

Conclusion

The work presented in this paper provides a comprehensive analysis of horizontal goal-oriented saccadic eye movements driven by an auditory and/or visual stimulus. Human saccadic responses to visual stimuli, auditory stimuli and auditory-visual bisensory stimuli are recorded by a high speed eye tracking system. The data is analyzed with a program written in FORTRAN programming language to compute parameter estimates for a horizontal saccadic eye movement models shown in Figures 2 and 4.

The auditory-visual stimuli provided the greatest saccade accuracy. Saccade peak velocity increases with increasing saccade amplitude and has an exponential shape. Auditory saccades show lower peak velocities and longer durations. Saccade latent period was relatively independent of saccade amplitude, but there is a significant reduction observed in the bisensory saccades. Auditory saccades exhibit lower agonist pulse magnitudes and longer agonist pulse durations for large saccades. Antagonist onset delay is longer in auditory saccades for the visual and auditory-visual bisensory saccades. A higher incidence of dynamic overshoot occurred in auditory saccades, more in the abducting direction than the adducting direction.

References

1. Bahill AT, Clark MR, Stark L (1975) The main sequence, a tool for studying human eye movements. Mathematical Biosciences 24: 191-204.
2. Enderle JD (1988) Observations on pilot neurosensory control performance during saccadic eye movements. Aviation, Space, and Environmental Medicine 59: 309-313.
3. Harwood MR, Mezey LE, Harris CM (1999) The spectral main sequence of human saccades. The Journal of Neuroscience 19: 9098-9106.
4. Enderle JD, Zhou W (2010) Models of horizontal eye movements. Part 2: A 3rd-order linear saccade model. Morgan & Claypool Publishers, San Rafael, CA.
5. Zhou W, Chen X, Enderle JD (2009) An updated time-optimal 3rd-order linear saccadic eye plant model. International Journal of Neural Systems 19: 309-330.
6. Enderle JD, Wolfe JW (1988) Frequency response analysis of human saccadic eye movements: estimation of stochastic muscle forces. Computers in Biology and Medicine 18: 195-219.
7. Enderle JD, Zhou W (2010) Models of horizontal eye movements. Part 1: Early models of saccades and smooth pursuit. Morgan & Claypool Publishers, San Rafael, CA.
8. Enderle JD, Sierra DA (2013) A new linear muscle fiber model for neural control of saccades. International Journal of Neural Systems 23.
9. Enderle JD (2002) Neural control of saccades. Progress in Brain Research 140: 21-49.
10. Ghahari A, Enderle JD (2014) A Physiological Neural Controller of a Muscle Fiber Oculomotor Plant in Horizontal Monkey Saccades. ISRN Ophthalmology 2014.
11. Ghahari A, Enderle JD (2014) A Neuron-Based Time-Optimal Controller of Horizontal Saccadic Eye Movements. International Journal of Neural Systems 24.
12. Ghahari A, Enderle JD (2014) Models of horizontal eye movements: Part 3, A neuron and muscle based linear saccade model. Morgan & Claypool Publishers, San Rafael, CA.
13. Ghahari A, Enderle JD (2015) Models of horizontal eye movements: Part 4, A multiscale neuron and muscle fiber-based linear saccade model. Morgan & Claypool Publishers, San Rafael, CA.
14. Gabriel DN, Munoz DP, Boehnke SE (2010) The eccentricity effect for auditory saccadic reaction times is independent of target frequency. Hearing Research 262: 19-25.
15. Frens M, Van Opstal AJ (1995) A quantitative study of auditory-evoked saccadic eye movements in two dimensions. Experimental Brain Research 107: 103-117.
16. Engelken EJ, Stevens KW, Enderle JD (1991) Relationships between manual reaction time and saccade latency in response to visual and auditory stimuli. Aviation, Space, Environmental Medicine 62: 315-318.
17. Lueck C, Crawford T, Savage C, Kennard C (1990) Auditory-visual interaction in the generation of saccades in man. Experimental Brain Research 82: 149-157.
18. Zahn JR, Abel L, Dell'Osso L (1978) Audio-ocular response characteristics. Sensory Processes 2: 32-37.
19. LaCroix TP, Enderle JD, Engelken EJ (1990) Temporal characteristics of saccadic eye movements induced by auditory stimuli. Biomedical Sciences Instrumentation 26: 67-77.
20. Engelken EJ, Stevens KW (1989) Saccadic eye movements in response to visual, auditory, and bisensory stimuli. Aviation, Space, Environmental Medicine 60: 762-768.
21. Zambarbieri D, Schmid R, Magenes G, Prablanc C (1982) Saccadic responses evoked by presentation of visual and auditory targets. Experimental Brain Research 47: 417-427.
22. Bell AH, Meredith MA, Van Opstal AJ, Munoz DP (2005) Crossmodal integration in the primate superior colliculus underlying the preparation and initiation of

saccadic eye movements. Journal of Neurophysiology 93: 3659-3673.

23. Corneil BD, Van Wanrooij M, Munoz DP, Van Opstal AJ (2002) Auditory-visual interactions subserving goal-directed saccades in a complex scene. Journal of Neurophysiology 88: 438-454.

24. Enderle JD, Wolfe JW (1987) Time-optimal control of saccadic eye movements. IEEE Transactions on Biomedical Engineering 34: 43-55.

25. Zhai X, Ghahari A, Enderle JD (2013) Characteristics of auditory and visual elicited saccades. Proceedings of the 39th Annual Northeast Bioengineering Conference (NEBEC), Syracuse, NY.

26. Zhai X, Ghahari A, Enderle JD (2013) Parameter estimation of auditory saccades and visual saccades. Proceedings of the 39th Annual Northeast Bioengineering Conference (NEBEC), Syracuse, NY.

27. Sparks DL (1986) Translation of sensory signals into commands for control of saccadic eye movements: role of primate superior colliculus. Physiol Rev 66: 118-171.

28. Sparks D (1988) Population coding of saccadic eye movements by neurons in the superior colliculus. Nature 332: 357-360.

29. Jay MF, Sparks DL (1987) Sensorimotor integration in the primate superior colliculus. I. Motor convergence. Journal of Neurophysiology 57: 22-34.

30. Meredith MA, Stein BE (1986) Visual, auditory, and somatosensory convergence on cells in superior colliculus results in multisensory integration. Journal of Neurophysiology 56: 640-662.

31. Stein BE, Stanford TR (2008) Multisensory integration: current issues from the perspective of the single neuron. Nature Reviews Neuroscience 9: 255-266.

32. Wallace MT, Stein BE (2001) Sensory and multisensory responses in the newborn monkey superior colliculus. The Journal of Neuroscience 21: 8886-8894.

33. Wallace MT, Perrault TJ Jr, Hairston WD, Stein BE (2004) Visual experience is necessary for the development of multisensory integration. The Journal of Neuroscience 24: 9580-9584.

34. Wallace MT, Wilkinson LK, Stein BE (1996) Representation and integration of multiple sensory inputs in primate superior colliculus. Journal of Neurophysiology 76: 1246-1266.

35. Populin LC, Yin TC (2002) Bimodal interactions in the superior colliculus of the behaving cat. The Journal of Neuroscience 22: 2826-2834.

This article was originally published in a special issue, **Design of Biosensors** handled by Editor. Dr. Eduardo De Faria Franca, Federal University of Uberlandia